Int. J. Bio-Inorg. Hybr. Nanomater., 5(1): 27-31, Spring 2016

Low temperature hydrothermal synthesis, characterization and optical properties of $Sr_6Nb_{10}O_{30}$ – Nb_2O_5 nanocomposite

Sh. Khademinia[1]; M. Behzad[1*]; A. Alemi[2]; M. Dolatyari[3]

[1] Department of Chemistry, Semnan University, Semnan 35351-19111, Iran
[2] Department of Inorganic Chemistry, Faculty of Chemistry, University of Tabriz, Tabriz, Iran
[3] SP-EPT Labs, ASEPE Company, Industrial Park of Advanced Technologies, 5364196795, Tabriz, Iran

Received: 1 December 2015; Accepted: 3 February 2016

ABSTRACT: $Sr_6Nb_{10}O_{30}$–Nb_2O_5 nanocomposite was synthesized in 2M NaOH aqueous solution. A stoichiometric 1:1 Sr:Nb molar ratio hydrothermal method at 120°C was used to synthesize this nanocomposite. $Sr(NO_3)_2$ and Nb_2O_5 were used as raw materials. The synthesized nanomaterials were characterized by powder X-ray diffraction (PXRD) technique. It was found that $Sr_6Nb_{10}O_{30}$ was crystallized in tetragonal crystal structure with space group P4/mbm and cell parameters of a = b = 12.3548 and c = 3.896 Å. Nb_2O_5 crystals were also found in orthorhombic and monoclinic crystal structures. Nb_2O_5 lattice parameters were found as a= 6.175 Å, b= 29.175 Å, c= 3.93 Å and a= 12.73 Å, b= 5.56 Å, c= 4.88 Å with γ= 105.1°, respectively for the orthorhombic and monoclinic crystal structures. The morphologies of the synthesized materials were studied by field emission scanning electron microscope (FESEM). The FESEM images showed that the synthesized nanocomposite had flower and sponge-like morphologies. Ultraviolet–Visible (UV-Vis) spectra showed that the synthesized nanocomposite had strong light absorption in the ultraviolet light region. FTIR spectrum of the obtained nanomaterial was also studied.

Keywords: *Crystal Structure; Hydrothermal Method; Nanocomposite; Optical property; $Sr_6Nb_{10}O_{30}$*

INTRODUCTION

Sr-Nb-O compounds such as other similar compounds are of interest for their wide range industrial applications and interesting properties (Shan, *et al.*, 2013). The compounds are ferroelectric material and have found several applications as a nonvolatile ferroelectric memory (Fujimori, *et al.*, 1998), optical waveguides (Ishitani, *et al.*, 1976) and a variety of other applications (Nanamatsu, *et al.*, 1975, Akishige, *et al.*, 2003). Photo catalytic water splitting reaction has also been studied extensively using these materials as photo catalyst under ultraviolet (UV) irradiation (Kato, *et al.*, 2003, Hwang, *et al.*, 2000, Machida, *et al.*, 2000, Kudo, *et al.*, 2000, Domen, *et al.*, 2001). We have recently reported the synthesis of $Sr_5Nb_4O_{15}$-Nb_2O_5 nanocomposites using a 1:2 molar ratio of Sr:Nb at different KOH concentrations which have some interesting applications (Khademinia and Behzad, 2015). However, $Sr_6Nb_{10}O_{30}$

(*) Corresponding Author - e-mail: mbehzad@semnan.ac.ir

is interested for its physical properties, including superconductivity, anisotropic conductivity, pseudo-one-dimensional crystal structure and low d-electron concentration (Hwang and Kwon., 1997). To the best of our knowledge, there is only two reported touts that have been conducted for the synthesis of $Sr_6Nb_{10}O_{30}$ which are two different solid state methods (Hwang and Kwon, 1997, Isawa, *et al.*, 1993). In the present study, a hydrothermal route was employed for the synthesis of nanostructured powder $Sr_6Nb_{10}O_{30}$ – Nb_2O_5 composite using $Sr(NO_3)_2$, Nb_2O_5 and NaOH as raw materials at 1:1 Sr:Nb molar ratio. The direct band gap energy of the as-prepared nanocomposite was initially estimated from UV-Visible spectrum. Besides, FTIR spectrum of the synthesized nanocomposite was also studied.

EPERIMENTAL

Materials and methods

All chemicals including $Sr(NO_3)_2$, Nb_2O_5 and NaOH were of analytical grade and were obtained from commercial sources (Merck, Germany) and were used without further purifications. Phase identifications were performed on a powder X-ray diffractometer D5000 (Siemens AG, Munich, Germany) using CuKα radiation. The morphology of the obtained materials was examined with a field emission scanning electron microscope (Hitachi FE-SEM model S-4160). Absorption spectrum was recorded on a Jena Analytik Specord 40 (AnalytikJena UK, Wembley, UK). Also, FTIR spectrum was recorded on a Tensor 27 (Bruker Corporation, Germany).

Hydrothermal synthesis of $Sr_6Nb_{10}O_{30}$-Nb_2O_5 nanocomposites

In typical synthetic experiment, 0.32 g (1.5 mmol) of $Sr(NO_3)_2$ (Mw = 211.62 g mol^{-1}) and 0.20 g (0.75 mmol) of Nb_2O_5 (Mw = 265.82 g mol^{-1}) were added to 50 mL of aqueous solution of 2 M NaOH under magnetic stirring at 80°C. The resultant solution was stirred for further 15 min and transferred into a 100 mL Teflon lined stainless steel autoclave. The autoclave was sealed and heated at 120°C for 48 h. When the reaction was completed, it was cooled to room temperature by water immediately. The prepared powder was washed with distilled water and dried at 120°C for 20 min under normal atmospheric condition. The obtained powder was placed in a 25 mL crucible and treated thermally at 400°C for 3 h. After the reaction was completed, the sample was cooled down naturally to the room temperature. The obtained nano powder was collected without any pulverization and used for further analyses.

RESULTS AND DISCUSSION

Powder X-ray diffraction analysis

The X-ray diffraction pattern of the $Sr_6Nb_{10}O_{30}$–Nb_2O_5 nanocomposite with the JCPDS card numbers are shown in Fig. 1. The results showed that the

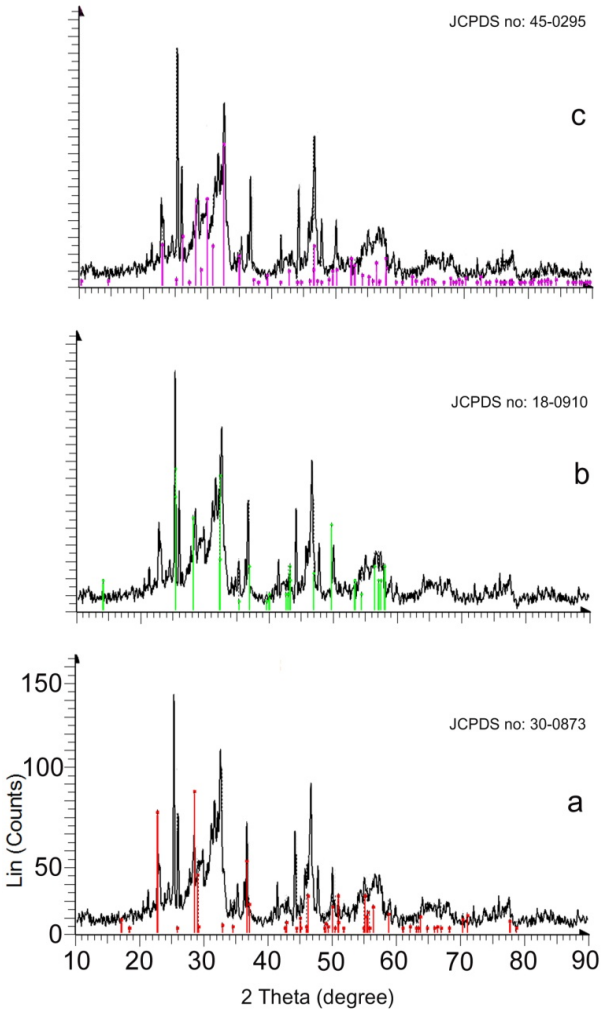

Fig. 1. PXRD pattern of the $Sr_6Nb_{10}O_{30}$ – Nb_2O_5 nanocomposite, the bars show the Bragg's positions for a) orthorhombic Nb_2O_5, b) monoclinic Nb_2O_5 and c) $Sr_6Nb_{10}O_{30}$.

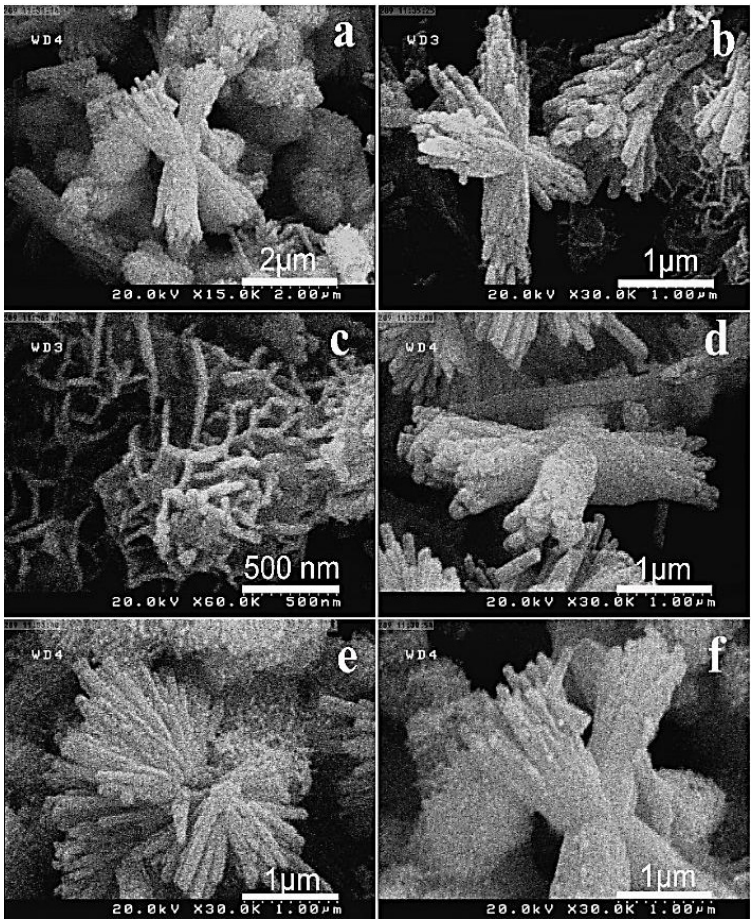

Fig. 2. FESEM images of $Sr_6Nb_{10}O_{30}$–Nb_2O_5 nanocomposite.

pattern had two main phases as $Sr_6Nb_{10}O_{30}$ and Nb_2O_5. As shown in Figs. 1a and 1b, two different crystal structures were observed for Nb_2O_5, namely orthorhombic and monoclinic crystal structures, respectively. Nb_2O_5 lattice parameters were found as a= 6.175 Å, b= 29.175 Å, and c= 3.93 Å for the orthorhombic phase; and a= 12.73 Å, b= 5.56 Å, and c= 4.88 Å with γ= 105.1° for the monoclinic phase. As shown in Fig. 1c, $Sr_6Nb_{10}O_{30}$ structure was detected with tetragonal crystal structure which has been crystallized in the P4/mbm space group. $Sr_6Nb_{10}O_{30}$ lattice parameters were found as a = b = 12.35 Å and c = 3.90 Å with α = β = γ = 90°. According to the PXRD pattern, it is clearly seen that the $Sr_6Nb_{10}O_{30}$ phase formation is comparable with that for Nb_2O_5.

Morphology of the obtained material

Figs. 2a-f show typical FESEM images of the hydrothermally synthesized $Sr_6Nb_{10}O_{30}$–Nb_2O_5 nanocomposite. From the typical FESEM images in Figs. 2a-c, it was found that the compound had a mixture of sponge and flower-like morphologies. These flowers were made of rods joint to each other to make a uniform structure. Fig. 2c shows that the thickness sizes of

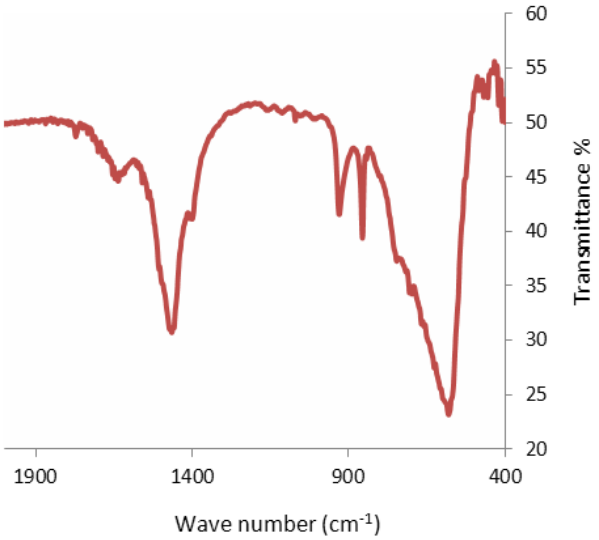

Fig. 3. FTIR spectra of $Sr_6Nb_{10}O_{30}$–Nb_2O_5 nanocomposite.

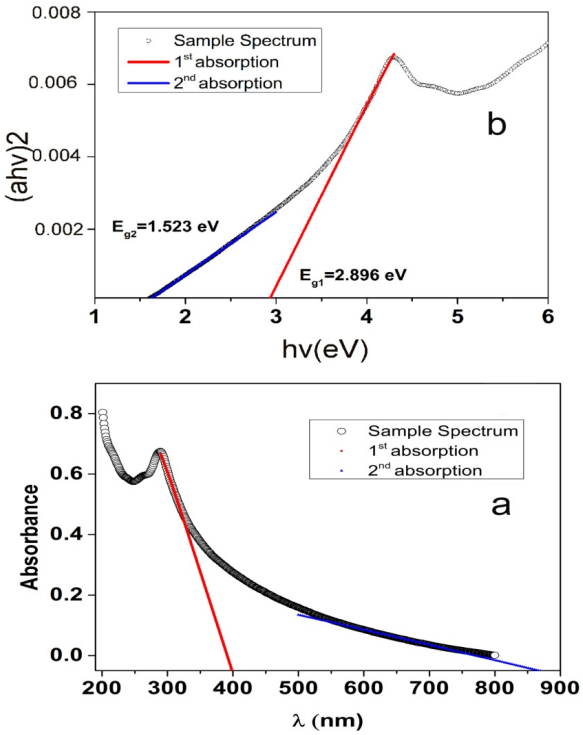

Fig. 4. Plots of a) UV-Vis spectrum and b) $(ahv)^2$ versus hv for $Sr_6Nb_{10}O_{30}$–Nb_2O_5 nanomaterial.

the sponge's sheets were about 40-50 nm. Figs. 2e-f shows that the rod diameters were about 100 nm.

Fig. 3 shows the FTIR spectrum of the synthesized $Sr_6Nb_{10}O_{30}$–Nb_2O_5 nanocomposite. This Fig. shows the absorption bands for $Sr_6Nb_{10}O_{30}$–Nb_2O_5 nanocomposite. The bands at around 636 and 854 cm^{-1} were assigned to monoclinic Nb_2O_5 and the bands at around 572 cm^{-1} was attributed to orthorhombic Nb_2O_5 (Ikeya, *et al.*, 1988, Ristic, *et al.*, 2004, Brayner, *et al.*, 2003, Jehng and Wachs, 1991). It is a confirmation of the co-existence of both orthorhombic and monoclinic Nb_2O_5 in the synthesized nanocomposite that is in agreement with the measured PXRD data. According to the spectrum, the peaks at 732, 854 and 925 cm^{-1} were corresponded to Nb-O vibrations (Khademinia and Behzad, 2015). The band at around 611 cm^{-1} was assigned to Sr–O vibration (Kamba, *et al.*, 2001, Angel, *et al.*, 2013).

UV-Vis spectrum and band gap calculation data are shown in Figs. 4a and 4b, respectively. $Sr_6Nb_{10}O_{30}$ – Nb_2O_5 nanocomposite displayed typical visible absorption edges at about 397 and 868 nm. According to the results of Pascual *et al.* (Pascual, *et al.*, 1978), the relation between the absorption coefficient and incident photon energy could be written as $(\alpha h\nu)^2 = A(h\nu - Eg)$, where A and Eg are constant and direct band gap energies, respectively. Band gap energy was evaluated by extrapolating the linear part of the curve to the energy axis. It was found that the band gaps were 1.5 and 2.9 eV.

CONCLUSIONS

In this work, $Sr_6Nb_{10}O_{30}$ – Nb_2O_5 nanocomposite was synthesized via a hydrothermal method. PXRD analysis confirmed the successful synthesis of the mentioned material. FESEM images showed that the as-synthesized nanomaterial had a mixture of plus, sponge and flower like morphologies. UV-Vis and FTIR spectra of the synthesized nanocomposite were also investigated and the band gap energies were calculated. It was found that the direct band gap was 2.896 eV.

REFERENCES

Shan L., Li W., Fang R., Han Z., Xu H., Dong L., Wu Z., Zhang X., (2013). Microstructure of strontium barium niobate/strontium barium titanate composite ceramics by powder–sol method. J. Inorg. Organomet. Polym., 23 (4): 855-860.

Fujimori Y., Izumi N., Nakamura T., Kamisawa A., (1998). Jpn. J. Appl. Phys. 37: 5207-5210.

Ishitani A., Kimura M., (1976). Single-crystal $Sr_2Nb_2O_7$ film optical waveguide deposited by rf sputtering. Appl. Phys. Lett., 29: 289-291.

Nanamatsu S., Kimura M., Kawamura T., (1975). Crystallographic and Dielectric Properties of Ferroelectric $A_2B_2O_7$ (A= Sr, B= Ta, Nb) Crystals and Their Solid Solutions. J. Phys. Soc. Jpn., 38: 817-824.

Akishige Y., Kamata M., Fukano K., (2003). Successive Phase Transition of $(Sr_{1-x}Ba_x)_2Nb_2O_7$. J. Korean. Phys. Soc., 42: 1187-1191.

Kato H., Kudo A., (2003). Photocatalytic Decomposition of Pure Water into H_2 and O_2 over $SrTa_2O_6$ Prepared by a Flux Method. Chem. Lett., 28: 1207-1208.

Hwang D.W., Kim H.G., Kim J., Cha K.Y., Kim

Y.G., Lee J.S., (2000). Photocatalytic Water Splitting over Highly Donor-Doped (110) Layered Perovskites. J. Catal., 193: 40-48.

Machida M., Yabunaka J., Kijima T., (2000). Synthesis and Photocatalytic Property of Layered Perovskite Tantalates, $RbLnTa_2O_7$ (Ln = La, Pr, Nd, and Sm). Chem. Mater., 12 (3): 812-817.

Kudo A., Kato H., Nakagawa S., (2000). Water Splitting into H_2 and O_2 on New $Sr_2M_2O_7$ (M = Nb and Ta) Photocatalysts with Layered Perovskite Structures: Factors Affecting the Photocatalytic Activity. J. Phys. Chem. B, 104 (3): 571-575.

Domen K., Kondo J.N., Hara M., Takata T., (2001). Photo- and Mechano-Catalytic Overall Water Splitting Reactions to Form Hydrogen and Oxygen on Heterogeneous Catalysts. Bulletin. Chem. Soc. Jpn., 73 (6): 1307-1331.

Khademinia S., Behzad M., Alemi A., Dolatyari M., (2015). Low temperature hydrothermal synthesis and characterization and optical properties of $Sr_5Nb_4O_{15}$ – Nb_2O_5 nanocomposite. Int. J. Bio-Inorg. Hybr. Nanomater., 4 (1): 49-54.

Hwang Y.K., Kwon Y.U., (1997). Syntheses and electrical properties of tetragonal tungsten bronze type solid solution Ba6 − xLaxNb$_{10}$O$_{30}$ + δ(x = 0, 1, 2, 3) and $Sr_6Nb_{10}O_{30}$. Mater. Res. Bull., 32 (11): 1495-1502.

Isawa K., Sugiyama J., Matsuura K., Nozaki A., Yamauchi H., (1993). Synthesis and transport properties of Sr_xNbO_3. Phys. Rev. B, 47: 2849-2853.

Ikeya T., Senna M., (1988). Change in the structure of niobium pentoxide due to mechanical and thermal treatments. J. Non-Cryst. Solid, 105: 243-250.

Ristic M., Popovic S., Music S., (2004). Sol–gel synthesis and characterization of Nb_2O_5 powders. Mater. Lett., 58: 2658-2663.

Brayner R., Verduraz F.B., (2003). Niobium pentoxide prepared by soft chemical routes: morphology, structure, defects and quantum size effect. Phys. Chem. Chem. Phys., 5: 1457-1466.

Jehng J.M., Wachs I.E., (1991). Structural chemistry and Raman spectra of niobium oxides. Chem. Mater., 3 (1): 100-107.

Khademinia S., Behzad M., (2015). Low temperature hydrothermal synthesis, characterization and optical properties of strontium pyroniobate. Adv. Powder Tech., 26: 644-649.

Kamba S., Petzelt J., Buixaderas E., Haubrich D., Vanek P., (2001). High frequency dielectric properties of $A_5B_4O_{15}A_5B_4O_{15}$ microwave ceramics. J. Applied Phys., 89: 3900-3906.

Angel J., Greena M., Karuppasamy K., Antony R., Shajan X. S., Kumaresan S., (2013). Effect of Magnesium Doping on the Physicochemical Properties of Strontium Formate Dihydrate Crystals. Chem. Sci. Trans, 2 (1): 141-146.

Pascual J., Camassel J., Mathieu M., (1978). Fine structure in the intrinsic absorption edge of TiO_2. Phys. Rev. B, 18: 5606-5614.

AUTHOR (S) BIOSKETCHES

Shahin KHademinia, Ph.D., Department of Chemistry, Semnan University, Semnan 35351-19111, Iran

Mahdi Behzad, Associate Professor, Department of Chemistry, Semnan University, Semnan 35351-19111, Iran, *E-mail: mbehzad@semnan.ac.ir, mahdibehzad@gmail.com*

Abdolali Alemi, Professor, Department of Inorganic Chemistry, Faculty of Chemistry, University of Tabriz, Tabriz, Iran

Mahboubeh Dolatyari, Associate Professor, SP-EPT Labs, ASEPE Company, Industrial Park of Advanced Technologies, 5364196795, Tabriz, Iran